INT. J. REMOTE SENSING, 1992, VOL. 13, NO. 2, 319–335

# Detection of circular structures on satellite images

H. TAUD

Faculté des Sciences, Université Mohammed V, Département de Physique, Laboratoire L.E.T.S., Avenue Ibn Battouta, BP 1014, Rabat Agdal, Maroc

J.-F. PARROT

Université Pierre et Marie Curie, Paris VI, Département de Géotectonique, 4, place Jussieu, Tour 26, 75230 Paris Cedex 05, France

*(Received 15 June 1989; in final form 11 June 1990)*

**Abstract.** An unsupervised method is proposed for detecting circular structures on satellite images partly based on a version of the Hough Transform. This method consists of two major steps: the extraction of significant contours from the image, using mathematical morphology operators, and the detection of circular structures from the contours previously defined. The latter includes four substeps: individualization of the curves, decomposition of the curves into near-circular elements, application of the 'adaptive HT' version to each near-circular element, and computation of more precise results. As an example, the method is applied to a SPOT scene in Southern Peru to detect geological structures.

## 1. Introduction

This paper is concerned with the detection of near-circular geological structures on SPOT satellite images using an unsupervised method. The near-circular structural features that can be observed on satellite images are the result often of geological phenomena. These phenomena may be meteoric (impact craters), magmatic and/or volcanic (volcanic cones, ring dykes, laccolites, batholites, annular intrusions, metamorphic aureoles, etc.), tectonic (periclinal terminations, conic folds, etc.), or sedimentologic, diapiric, etc.

The Hough Transform (Hough 1962) is a method for detecting complex shapes on a binary image. Several versions were proposed and applied in different fields (Duda and Hart 1972, Ballard 1981, Tsuji and Masumoto 1978, Casasent and Krishnapuram 1987). In order to detect circular shapes, a version of the Hough Transform was proposed by Kimme *et al.* (1975) and improved by Gerig and Klein (1986). This version was recently used by Cross (1988) for detecting circular geological structures on a MSS Landsat image.

With the same objective, we have applied another version of the Hough Transform ('adaptive HT') developed by Illingworth and Kittler (1987) to a SPOT image. We tested the Illingworth–Kittler version on synthesized images corresponding to different circular geological structures, in order to check the reliability of the method. It is known to give satisfactory results when the circular shapes are more or less complete and when they are either isolated or concentric. However, in the case of incomplete circles or when the image includes several eccentric circles, or when the curves are formed by a succession of circular elements alternately convex and concave, the error rate is high.

In view of these results, the method proposed in this paper involves two main steps.

(*a*) The extraction of the significant contours from the satellite data. The major part of the processing related to this step is based on mathematical morphology (Serra 1982, Coster and Chermant 1985).

(*b*) The detection of circular structures from the significant contours. This step consists of four sub-steps:

(i) the individualization of the various features found in the image, using an algorithm based on the Freeman code (Freeman and Davis 1977);

(ii) the decomposition of each feature isolated at the previous step into near-circular elements, according to the change in the curvature direction;

(iii) the application of the 'adaptive HT' version to each near-circular element which yields approximate values for the centre and the radius of the element; the accuracy depends on the length of the circle arc;

(iv) the exploitation of the previous information by calculation which obtains precise results.

## 2. Extraction of significant contours

The first step of the processing is concerned with the extraction of the significant contours contained in the satellite image under study. The use of contour detection operators, such as the Sobel (Pratt 1978, Rosenfeld and Kak 1982) on the raw data of a satellite image does not directly lead to an improvement in the data which enables the second step to be processed. The wealth of information obtained with these operators requires a thresholding, which involves supervised processing.

The unsupervised processing proposed here is partly based on the use of several operators borrowed from mathematical morphology (refer to figure 1). We applied mathematical morphology under its two forms (binary and multilevel), in order to omit non-relevant information and to smooth the limits of the various objects present in the studied area. In both cases, the selected structuring elements are composed in a square raster.

In the first substep, the satellite image is applied a closing (dilation followed by an erosion), in order to fill in the holes, the channels and the interstices. This operation is followed by an opening (dilation following an erosion) which suppresses the isles and capes. The different levels of the resulting values are then distributed into two levels including an equivalent number of pixels (equipopulation technique), by means of an automatic thresholding of the reflectance histogram (substep 2). At this stage, a geodesic dilation (Coster and Chermant 1985) is performed, in order to suppress the holes contained in one of these two levels (substep 3).

Successive thinnings and prunings are applied to the resulting image based on the mask proposed by Lantuejoul (Coster and Chermant 1985). This operation is repeated until the number of pixels eliminated at each iteration becomes lower than the limit set at 1 per cent of the number of pixels extracted at the first application of the mask. Lastly, the isolated points are suppressed (substep 4).

The limits of the different shapes thus obtained, are traced by analysing the reflectance skips between two neighbouring pixels, according to two directions (NS and EW), in order to obtain the height-connected contour (substep 5). The absolute value of the difference between the levels of two neighbouring pixels is related either to the position of the pixel of the lower level, or to the position of the pixel of the higher level. If the studied object is coded with values higher than those of the

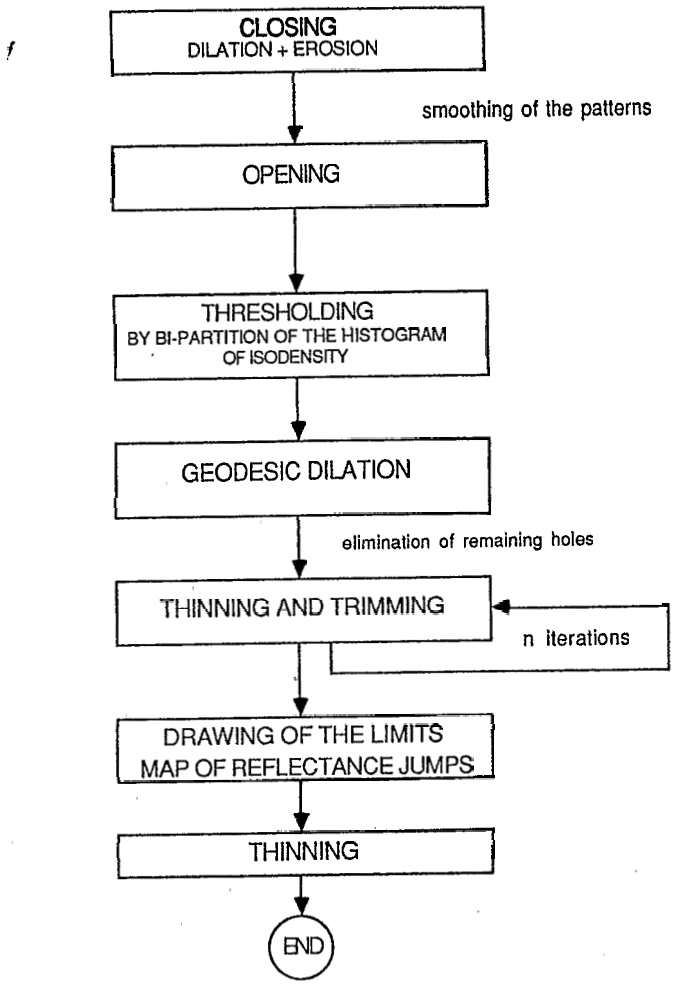


Figure 1. Unsupervised processing.

surroundings, it may be observed in the first case that the limit surrounds the shape, and in the second case that the limit exactly corresponds to the location of the pixels that outline the edge of the shape. This accuracy must be taken into consideration in order to compute the exact value of the radius of the circle detected on the satellite image.

The coded limit thus obtained is thinned at substep 6 so as to eliminate the right angle pixels sometimes generated by the preceding substep. All the structural features (secants or isolated straight lines or curves) revealed through this preliminary process are next treated by the method described hereafter.

## 3. Detection of the characteristics of the near-circular elements

The contours detected in the above step are recorded in a binary image. The method applied (refer to figure 2) to this image involves four substeps: individualization of the curves; decomposition of the curves into near-circular elements; application of the 'adaptive HT' version to each near-circular element; computation of more precise results.

3.1. *Individualization of the curves*

The curves are individualized by a contour following. The contour following is based on the movement of a sliding $3 \times 3$ pixel window $W_n$; the index $n$ indicates the position of the window on the $n$th pixel of the contour. The developed algorithm allows to decide which direction to follow whether a crossing occurs or not.

3.1.1. *Contour following*

The contour following operations are based on the Freeman code in eight directions. This encoding is an accurate representation of each pixel of the contour and uses the relative position of one contour pixel with respect to the preceding pixel. Methods based on this kind of closed contour following are well known (see for example, Toumazet 1987, p. 168). These methods cannot be applied, however, without modifying the satellite images whose contours are not always closed and which may show one or two 'ends of branch'. By this we mean the absence of a pixel connected to the central pixel in the last tested window. We were led therefore to develop the following procedure.

Let $P_c$ be the central pixel of a window $W_n$, and let $P_v$ be the pixel connected to the central pixel of the same window. The whole image is scanned line by a line from left to right. When a contour pixel is encountered, the $3 \times 3$ window $W_1$ centred on this pixel $P_c$ is tested; the test allows us to know whether only one possible direction exists

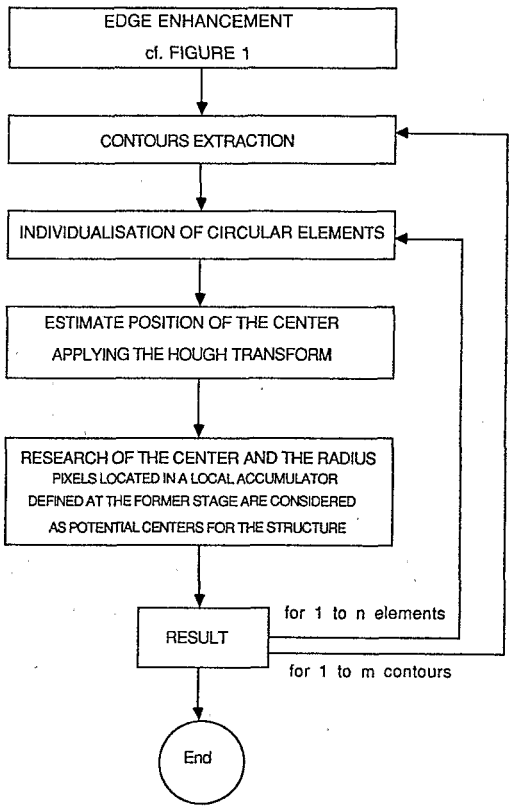


Figure 2. Detection of characteristics.

(only one neighbouring pixel), or whether there are several possible options (two neighbouring pixels). In the first case this means we are reaching the beginning of a non-closed contour (only one branch); in the second case, whether the scanning encounters a non-closed contour in any of its points or a closed contour. When the contour is not closed, the sliding window follows the contour to the end of the first branch, and then returns to $W_1$ to follow the second branch. When the contour is closed, the sliding window goes back to the starting point ($W_1$,) suppressing point-by-point the second branch during contour following.

Owing to the scanning direction and to the skeletonization performed at the first step, only six possibilities may occur in the window $W_1$ (figure 3).

(*a*) Only one connected point. We are in the presence of the extremity of a non-closed contour. The connected pixel indicates which of the four directions to follow. Contour following begins and goes on until the other extremity is reached (end of branch).

(*b*) Two connected points. In this case, the pixel encountered corresponds to a contour either closed or not. One of the connected pixel ($P_{v1}$) is always located in the south-west corner (code 7); the second ($P_{v2}$) is either in the south-east corner (code 5) or on the right of the central pixel (code 4). The first move is directed towards the lower left-hand pixel of the window $W_1$ (code 7), but the existence of a second direction (code 4 or code 5) is stored in memory, in order to resume the contour following at this point, if the first direction reaches the end of a branch (non-closed contour).

3.1.2. *Crossings*

As contour following proceeds, the sliding window goes from position $W_n$ to position $W_{n+1}$. The central pixel of the window $W_{n+1}$ is eliminated in order not to be considered while the window $W_{n+1}$ is tested. The code of the direction chosen in the window $W_n$ is stored in the memory so as to be matched with the code of the direction selected in the window $W_{n+1}$, whenever necessary.

As stated above, the absence of a connected pixel in a window corresponds to an 'end of branch'. We may possibly come back to the very first pixel ($P_c W_1$) encountered during the image scanning, if two connected pixels were associated with this first pixel.

In case only one connected pixel is found in the window $W_{n+1}$, we keep on following the contour. On the other hand, when the number of the connected pixels

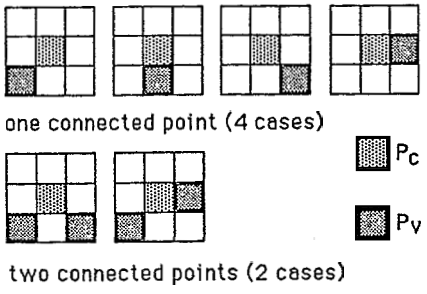


Figure 3. The six possibilities found in the first window.

found in the window $W_{n+1}$ is higher than one, we are in presence of a crossing (three pixels), or even of a collateral branch (two pixels). Then, the window is moved according to the code of the direction selected in $W_n$ (figure 4). The decision to proceed in one of the different possible directions is based on the following general condition (condition 1): the absolute value of the difference between the code $C_n$ selected in $W_n$ and the code $C_{n+1}$ selected in $W_{n+1}$ must not exceed 1; i.e.

$$|C_n - C_{n+1}| \leq 1$$

This condition is necessary but not sufficient to continue contour following. The subsequent procedure depends on the number of connected pixels $P_v$ in the window $W_{n+1}$ which satisfy condition one.

When we are in the presence of connected pixels, the choice bears either on the sole pixel $P_v$ that satisfies condition 1 ($|C_n - C_{n+1}| \leq 1$), or on the pixel that satisfies condition 2 ($C_n - C_{n+1} = 0$) when the two or three pixels $P_v$ meet condition 1. However, when only two pixels $P_v$ satisfy condition 1 and none of them satisfy condition 2, that is when the two possible directions are situated symmetrically on either side of the direction selected in $W_n$, a test is applied in order to know which direction enables us to follow the contour. In this test the code of the first direction ($C_{n+1}$) corresponding to condition 1 in $W_{n+1}$ is added to the code of the direction $C_{n+2}$ found in $W_{n+2}$ were this direction followed. The same operation is performed

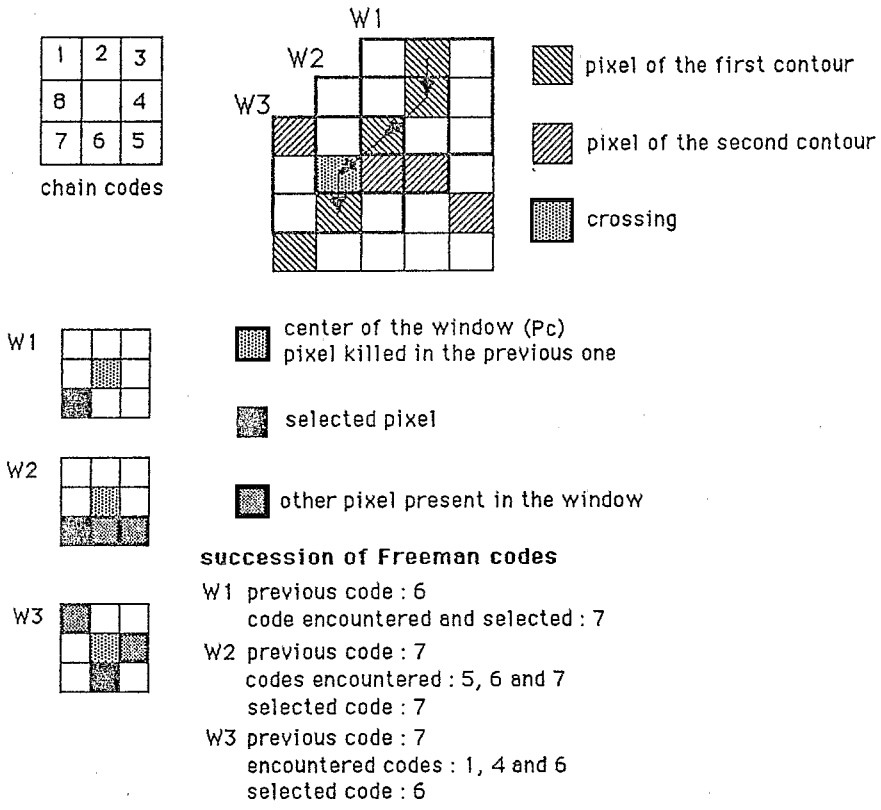


Figure 4. Decision making in case of crossing.

for the second possible direction. The two sums are compared with the sum of the two codes ($C_n$ and $C_{n-1}$) preceding the crossing encountered in the window $W_{n+1}$. The selected direction is such that $|(C_{n-1}+C_n)-(C_{n+1}+C_{n+2})|$ is the smallest. If the difference is identical in the two directions, it is possible to consider a higher number of codes. If $i$ is the number of codes taken into account on either side of the crossing pixel, as a general rule we may say that the selected direction is the one whose value $M$ is the lowest (condition 3).

$$M=|(C_{n-(i-1)}+C_{n-(i-2)}+\cdots+C_n)-(C_{n+1}+\cdots+C_{n+(i-1)}+C_{n+i})|$$

The value $i$ increases until a second crossing occurs, or an end of branch, or else when $i=n$. If condition 3 cannot be met before we reach the limit to which value $i$ can increase, the crossing found in $W_{n+1}$ is considered an end of branch. A correction is made when the codes 8 and 1 are matched. Note that condition 2 is a special case of condition 3.

When the end of a contour is detected, the crossing pixels, if any, are reactivated so as to ensure the continuity of the other contours still to be detected.

3.2. *Decomposition of the curves into near-circular elements*

The contours individualized at the previous step are sometimes formed by a succession of circular elements which are alternately convex and concave. This kind of structural feature is often found in the geological field.

In order to decompose the curve into near-circular elements, the points of inflection where a change in the curvature direction occurs have to be detected. In the discrete mode, we consider that a curve can be decomposed into a succession of straight lines consisting of 1 to $n$ pixels whose directions are either vertical or horizontal.

If we follow a circular section, the difference between two subsequent values of the Freeman code is equal to 1, 0 or $-1$ (figures 5 and 6). If we do not take the value 0 into account, we observe a regular alternation of 1 and $-1$ values. This pair of values ($1/-1$ or $-1/1$) marks the passage between two subsequent straight line segments of the curve, which remains identical as long as these subsequent segments remain horizontal (or vertical) and as long as the move along the perpendicular axis with respect to the direction of these segments does not change (figure 7).

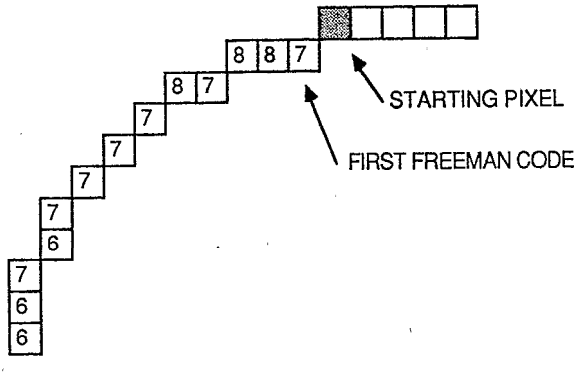


Figure 5. Succession of Freeman codes on a circular section.

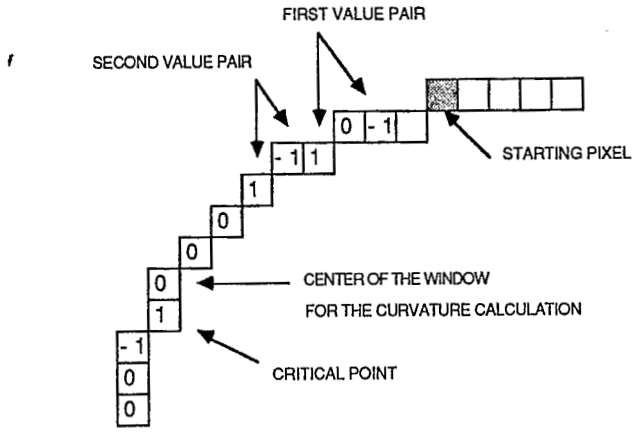


Figure 6. Differences between the Freeman codes recorded on the preceding figure.

A change in the movement described above, or a change in the direction of the segments (horizontal segments changing to vertical segments, or the opposite), leads to an inversion of the value of these pairs.

In terms of successive pairs of values, the phenomenon may have the following outlook:

$-1,1\ldots-1,1 \longrightarrow 1,-1$ (1st type)
pairs of opposite values — inverted pair of opposite values

$-1,1\ldots-1,1 \longrightarrow 1,1$ (2nd type)
pairs of opposite values — pair of identical values

The pixel ($P_{pc}$) where this phenomenon occurs is called a 'critical point'.

A critical point may correspond to a transition point of the curve which presents the same curvature (a complete circle contains eight critical points), or to a change in the curvature direction.

In order to find out whether or not a critical point corresponds to the transition from a convex curve to a concave curve, we examine the shape of the

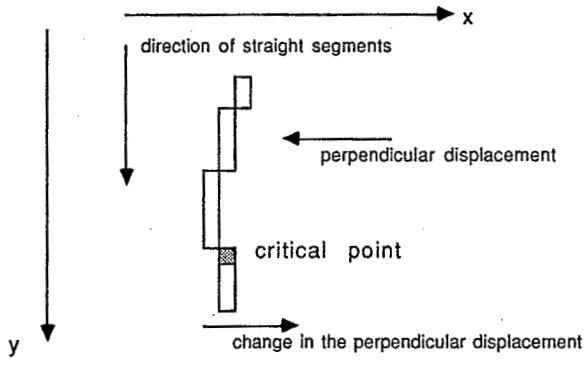


Figure 7. A critical point occurs when there is a change of direction perpendicular to the straight line segments direction.

curve about the critical point by means of the window $W_v$. The first window is centred on the starting pixel of the contour ($P_c$ of $W_1$). The subsequent windows are centred on the pixel preceding the critical point ($P_{pc}$). These windows are divided into two equal parts by a straight line (separating line) which passes through the centre of the window and contains the maximum number of contour pixels found in following one of the four directions: N–S, E–W, (NE)–(SW) or (NW)–(SE). This window is of variable size. It increases until there is no contour pixel left on the two end pixels of the separating line. For example, figure 8 shows that a window of size 9 by 9 is large enough to calculate the code of curvature.

At this stage, the pixels belonging to the considered contour which are not on the separating line are localized either on both sides of this line or on one side only.

The first localization implies a change of curvature directly noticeable on the window. The second one allows us to calculate the curvature direction. This curvature direction is coded in the same way as the Freeman code. The localization of the contour pixels on one of the eight regions possibly generated by the separating line, allows us to code the curvature direction at the critical point (figure 8). In the example shown in figure 8, the curvature direction is coded 1.

A contour is assumed to present a change of curvature, either when the contour pixels are distributed on both sides of the separating line, or when the absolute value of the difference between two successive codes exceeds 1. A correction is made when the codes 8 and 1 are matched.

### 3.3. *Hough Transform*

When a near-circular element is individualized by the preceding substep, a version of the Hough Transform (Illingworth and Kittler 1987) is applied in order to determine the approximate location of the centre of this element and the approximate value of its radius.

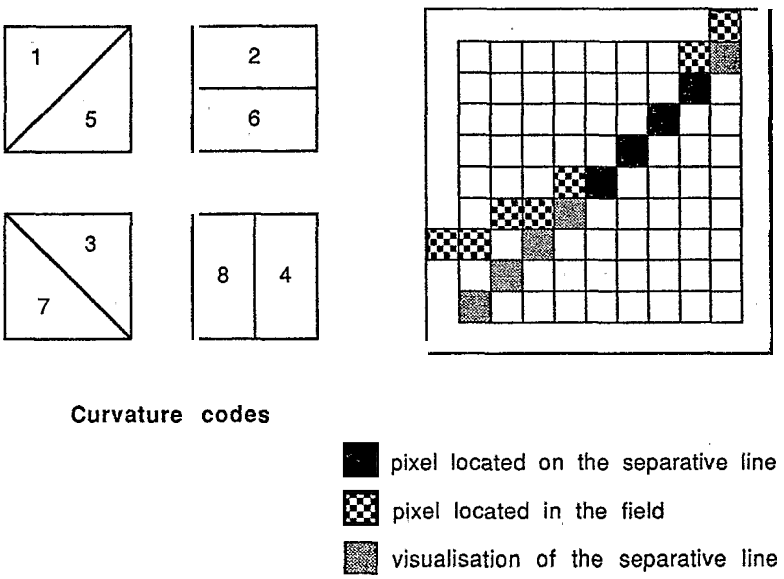


Figure 8. Codes and calculation of the curvature direction.

3.3.1. *Generalities*

The Hough Transform converts a complex problem of shape detection in image space into a peak detection problem which is easier to solve in parameter space. The Hough Transform may be generalized and specialized in various fields. Duda and Hart (1972) showed that this transform also enables us to detect circular lines.

The equation of a circle is defined in the following way:

$$(x-a)^2+(y-b)^2=r^2 \tag{1}$$

where $r$ is the circle radius and $(a, b)$ its centre. The Hough Transform maps each point of the contour onto the three-dimensional parameter space $(O, a, b, r)$. The latter is quanti and used as an 'accumulator' initialized at zero throughout.

Each point of image space which is mapped onto parameter space is transformed into a cone whose summit is at the point $(x, y, O)$ as indicated in figure 9 $(b)$. Indeed, (1), which defines a circle in image space (cf. figure 9 $(a)$), represents a conic surface of parameter space which satisfies the equation

$$(a-x)^2+(b-y)^2=(r-O)^2 \tag{2}$$

3.3.2. *Illingworth–Kittler version*

A high-dimension parametrization can often be decomposed into parametrizations of small dimension. This idea is extremely beneficial in terms of storage and computation requirements. Illingworth and Kittler (1987) propose a two-dimensional parametrization, instead of three parameters, to detect a circle, followed by a one-dimensional parametrization. In order to find the centre of the circle, the following constraint must be satisfied: all the vectors normal to the tangent at each point of the contour must intersect at the centre of the circle. The estimation of the normal direction may be obtained by local edge detection operators such as the Sobel.

Knowing the triple $(x, y, \theta)$ allows us to find the centre of the circle if $a$ and $b$ are its parameters (figure 10).

The mapping of each triple $(x, y, \theta)$ onto the two-dimensional space $(O, a, b)$ generates straight lines which satisfy the equation

$$b=tg\theta a+(y-xtg\theta) \tag{3}$$

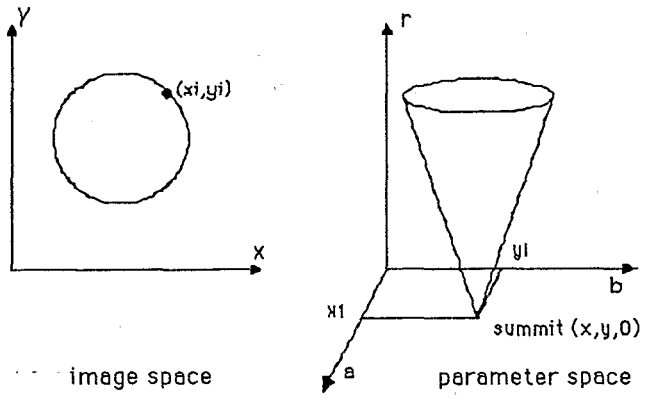


Figure 9. Hough Transform of a point belonging to the circle: $(a)$ image space, $(b)$ parameter space.

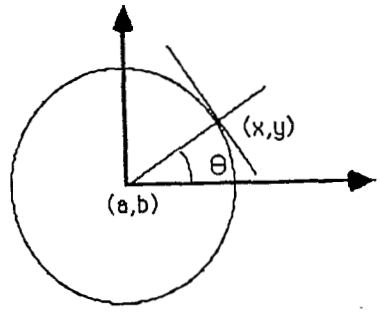


Figure 10. Relationship between $(x, y, \theta)$ and the centre parameters $(a, b)$.

where $\theta(x, y) = D(x, y) - \pi/2$ is the normal direction with $D(x, y)$ the Sobel direction.

The radius is found from the histogram $\delta = (x-a)^2 + (y-b)^2$, where $a$ and $b$ are the coordinates of the circle determined at the first step. The radius is identified as the highest peak of the histogram.

3.3.3. *Application of the Hough Transform*

The search for the maximum (or maxima) recorded into the accumulator leads to the detection of the circle centre, which is the locus where the highest number of normals intersect. The normal derivative proper to the discrete mode, produces a dispersion of the maxima about the central point, which leads to the notion of uncertainty; that is, the distance between centre calculated according to the lines (incy) and according to the columns (incx) and the maximum which is the most distant from the centre.

The centre is calculated from the two maxima most distant from one another according to the $x$-axis and according to the $y$-axis, respectively. The centre is localized half-way from these two maxima. In the discrete case, the notion of half-distance leads us to define the uncertainties incx1, incx2, incy1 and incy2. The coefficient of uncertainty inc corresponds to the maximum value of these uncertainties (figure 11).

The uncertainty is high when the near-circular structures are incomplete. The arcs generate in the accumulator a shift of the corresponding peak with respect to the real position of the centre.

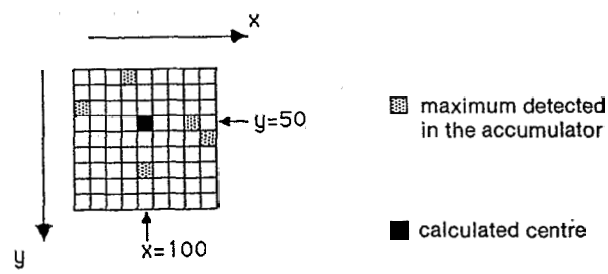


Figure 11. Calculation of the centre from the maxima detected in the accumulator.

3.4. *Finding the exact location of the centre*

With the Hough method, the detection of circular structures is essentially based on the contour pixels. Another approach consists of considering all the pixels which do not belong to the contour as probable centres of this contour. For each probable centre, the distance of the centre to each point of the contour is computed from

$$d=[(x_i-x_p)^2+(y_i-y_p)^2]^{1/2}$$

where $x_i, y_i$ represent the coordinates of a contour point, and $x_p, y_p$ the coordinates of a probable centre. Thus, for each probable centre we obtain a histogram containing, on the $x$-axis, the values of the distances, and on the $y$-axis the number of the distances found for each of these values.

The histogram maximum $\mathrm{Max}_p$ corresponds to the most frequent distance between the probable centre and the contour points. This distance $d_p$ is then considered as the radius value. The maximum $\mathrm{Max}_p$ together with the value of the corresponding distance $d_p$ are recorded as

$$M(x_p, y_p)=\mathrm{Max}_p \qquad \text{and} \qquad R(x_p, y_p)=d_p$$

When all the probable centres have been tested, the maximum found in the table $M(x_p, y_p)$ allows us to find the exact location of the centre of the contour under study. According to this location, the table $R(x_p, y_p)$ then provides the value of the related radius.

The probable centres of the circle are only tested in an area which surrounds the strong values in the accumulator. The selected area is a window whose size is determined by the inc value (Taud 1989); the window is centred on the approximate centre previously computed by the Hough Transform.

## 4. Example of an application to a SPOT image

The method described in this paper may be applied in numerous fields as well as to numerical images of various origins. We will take as an example, the search for circular structures in a SPOT image.

4.1. *Geological outline of the region under study*

The test area is located in the south-west of Peru, more precisely in the Arequipa district (figure 12). It is a volcanic zone essentially andesitic, situated in the Western Cordillera (Huaman-Rodrigo 1985, Vicente 1988). Strato-volcanoes of the Plio-quaternary era lie on a Mesozoic substratum. This region presents many near-circular structures due to the existence of volcanic cones, craters, flow fronts, as well as semicircular plucking zones.

4.2. *Processing and results*

The processed image (figure 13) is a SPOT scene acquired on 21 July 1986 (path 160–row 381; shot angle: 10° E). The near-infrared multispectral XS3 channel was selected because of its quality to bring out geological structures.

The method which, as seen above, involves two major steps, is applied to a 256 by 256 pixel subscene (lines: 51 to 306; columns: 1201 to 1456).

(*a*) first step. The raw data of the satellite image are applied a closing followed by an opening, and the different levels of values are distributed into two levels including an equivalent number of pixels. Next, a geodesic dilation is applied to one of these

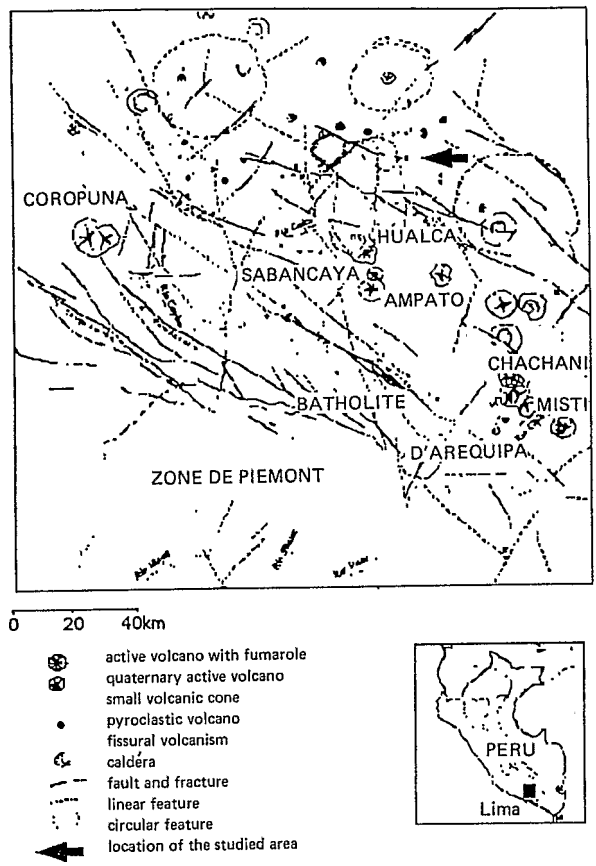


Figure 12. Schematic geological map of the region under study.

value levels so as to suppress the holes (figure 14); the dilation is followed by successive thinnings and prunings. The boundaries of the different shapes thus obtained are traced by analysing the reflectance changes and are next applied a thinning (figure 15).

(*b*) second step. The structural features revealed by the first step are processed in the second step, which allows us to detect circular structures from the significant contours. Each isolated structural feature is decomposed into near-circular elements, according to the changes occurring in the curvature direction; the 'adaptive HT' version is applied to each near-circular element, and additional computation provides more accurate results.

Thus, in the subscene under study two near-circular structures are distinguished among all the structural features present in the image (figure 16).

The locations of the centre and the value of the radius have been computed. The centre of the first structure is localized on column 1272 and line 174 of the complete SPOT scene; the radius is 26 pixels, which means a diameter of 1040 m. The second centre is located on column 1311 and line 250 of the SPOT scene; the radius is 18 pixels, that is, a 720 m diameter.

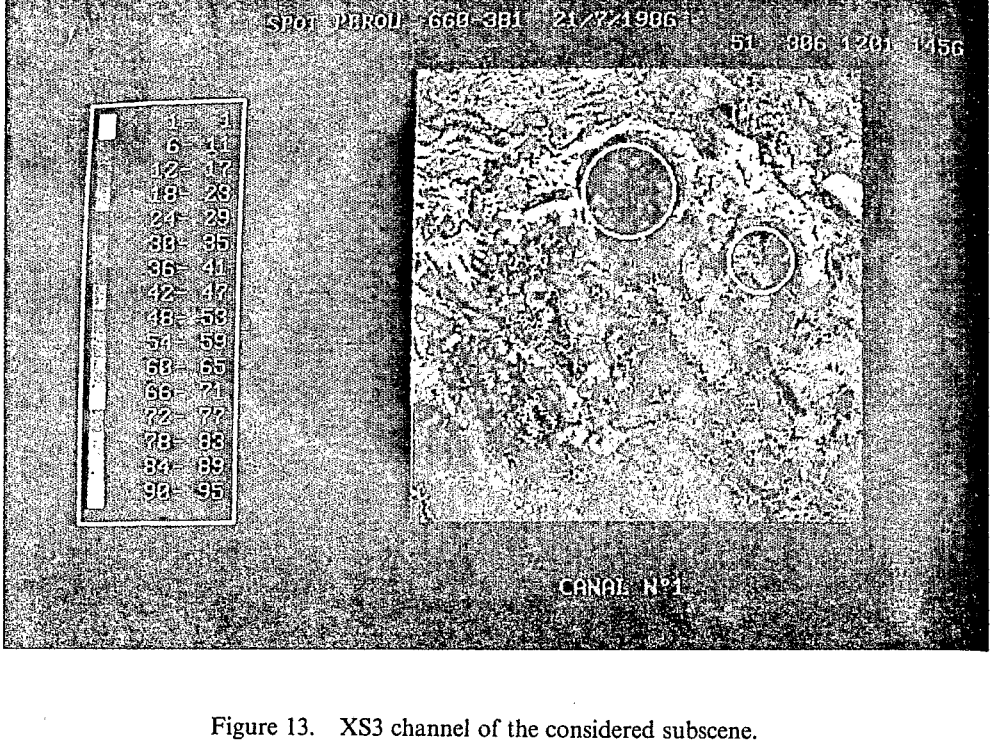


Figure 13. XS3 channel of the considered subscene.

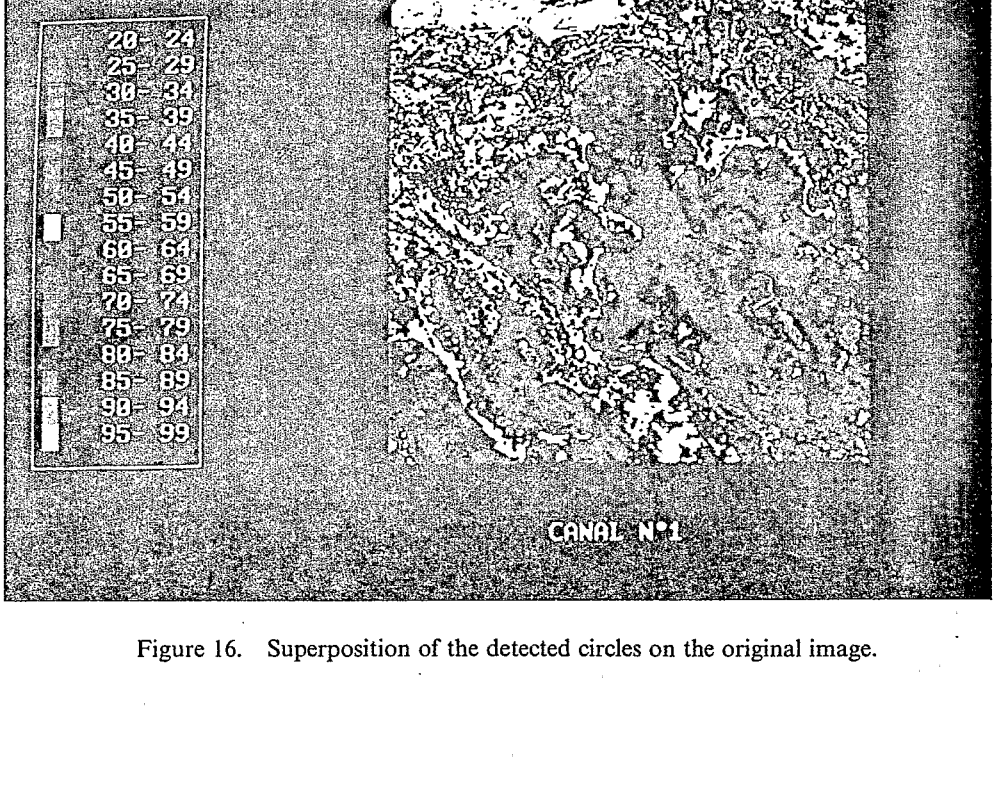


Figure 16. Superposition of the detected circles on the original image.

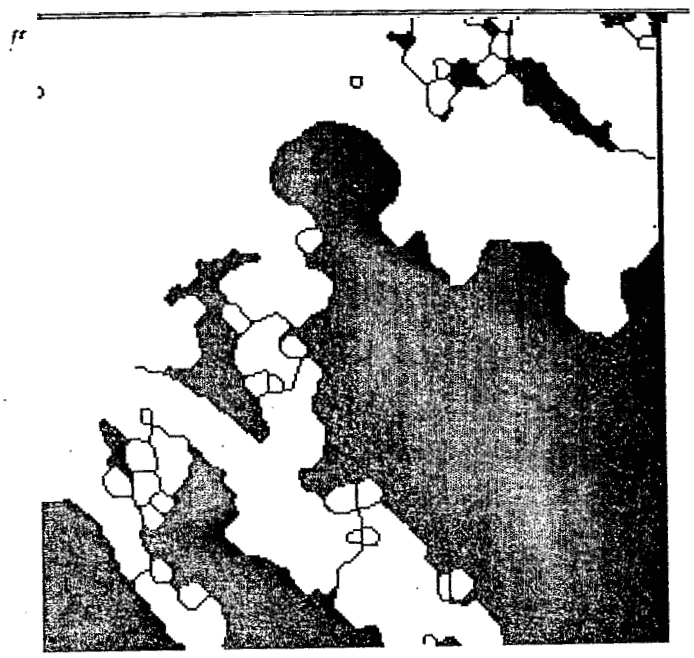

Figure 14. Bipartition of the scene by equipopulation followed by a geodesic dilation and thinnings.

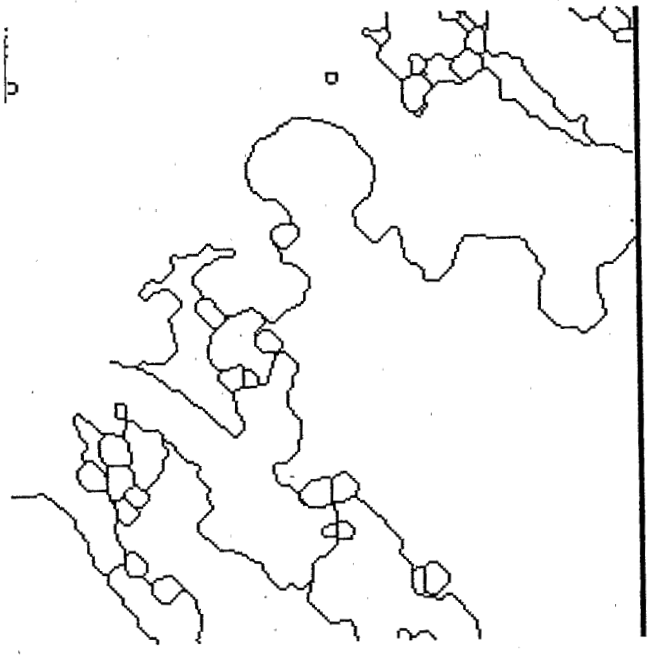

Figure 15. Extraction of the boundaries from figure 14.

In order to test the validity of these results, the number of pixels outlining the extracted structure is compared with the number of pixels of this structure that intersect those of the computed centre. In the first case, 38 per cent of the pixels of the near-circular structure belong to the circle, and 33 per cent in the second case. We may consider the 20 per cent is a reasonable lower limit, if we take into account the generally irregular shape of the detected contours.

## 5. Conclusion

The second step of the method developed in this paper may be applied in numerous fields (biological, geological, pedological, industrial, etc.). The whole of the method may concern numerical images of various origins (satellite data, numerical models, etc.). In the example of application we have chosen, circular geological structures are searched for in a SPOT image. In this field, many circular structures noticeable on satellite documents may be the result of subjective interpretation. The method developed here aims at an objective detection of these structures. The method is unsupervised and only includes a few constraints which may be set beforehand by the user. For example, a near-circular contour will be taken into account only beyond a certain number of pixels.

The proposed method consists of two major steps.

(*a*) Extraction of the significant contours from satellite data. This step is essentially based on mathematical morphology.

(*b*) Detection of circular structures from the significant contours. This step includes four sub steps:

(i) Individualization of the different features found in the image; this substep is based on the Freeman code and consists of following a contour and making a decision in case a crossing occurs.

(ii) Decomposition of each feature isolated at the previous substep into near-circular elements, according to the change in the curvature direction. To achieve this, the 'critical points' are examined in order to establish whether or not they correspond to an inflection point.

(iii) Application of the 'adaptive HT' version to each near-circular element; which provides, according to the number of intersections between the normals and the contour recorded in the 'accumulator', the approximate values of the centre and radius of the element.

(iv) Testing of all the pixels contained in the zone surrounding the maximum values found in the accumulator and considered as probable centres.

The results obtained by the application of the method to a SPOT image confirm the possibility of an unsupervised detection of circular structures. The unsupervised detection of near-circular structures on satellite data also open new prospects in the field of shape modelling and recognition.

## References

BALLARD, D. H., 1981, Generalizing the Hough Transform to detect arbitrary shapes. *Pattern Recognition*, **13**, 111–122.

CASASENT, D., and KRISHNAPURAM, R., 1987. Curved object location by Hough Transformations and invertions. *Pattern Recognition*, **20**, 267–276.

COSTER, M., and CHERMANT, J.-L., 1985, *Précis d'analyse d'images* (Paris: CNRS).

CROSS, A. M., 1988, Detection of circular geological features using the Hough Transform. *International Journal of Remote Sensing*, **9**, 1519–1528.

DUDA, R. O., and HART, P. E., 1972, Use of the Hough Transform to detect lines and curves in pictures. *Communications of the Association of Computing Machinists*, **15**, 204–208.

FREEMAN, H., and DAVIS, L. S., 1977, A corner-finding algorithm for chain coded curves. *I.E.E.E. Transactions on Computers*, **26**, 297–303.

GERIG, G., and KLEIN, F., 1986, Fast contour identification through efficient Hough Transform and simplified interpretation strategy. *8th International Joint Conference on Pattern Recognition, October 1986* (Paris: CNRS), pp. 498–500.

HOUGH, P. V. C., 1962, A method and means for recognizing complex patterns. V.S. Patent 3 069 654.

HUAMAN-RODRIGO, D., 1985, Evolution tectonique cenozoique et néotectonique du Piémont Pacifique dans la région d'Arequipa (Andes du Sud Pérou). Thèse 3ème cycle Université Paris XI.

ILLINGWORTH, J., and KITTLER, J., 1987, The adaptive Hough Transform. *I.E.E.E. Transactions on Pattern Analysis and Machine Intelligence*, **9**, 690–698.

KIMME, C., BALLARD, D., and SKLANSKY, J., 1975, Finding circles by an array of accumulator. *Communications of the Association of Computing Machinists*, **18**, 120–122.

PRATT, W. K., 1978, *Digital Image Processing* (New York: Wiley).

ROSENFELD, A., and KAK, A. C., 1982, *Digital Picture Processing* (New York, London: Academic Press).

SERRA, J., 1982, 1988, *Image Analysis and Mathematical Morphology* (London, New York: Academic Press).

TAUD, H., 1989, Detection des structures circulaires sur image numérique: recherche non supervisée des structures géologiques sur image satellitaire. Thesis 3ème cycle Université Mohammed V, Rabat.

TOUMAZET, J.-J., 1987, *Traitement de L'image sur Micro-ordinateur*. (Paris: Sybex Ed.).

TSUJI, S., and MATSUMOTO, F., 1978, Detection of ellipse by modified Hough transformations. *I.E.E.E. Transactions on Computers*, **22**, 777–781.

VICENTE, J. C., 1988, Early Late-Cretaceous overthrusting in the western cordillera of southern Peru. In *Geology of the Andes and its Relation to Hydrocarbon and Mineral Resources*, edited by Ericksen *et al.* (Earth Science Series, Vol. 11, Chapter 6) (Houston, Texas: Circum-Pacific Council for Energy and Mineral Resources), 91–117.